Transactions on Additive Manufacturing Meets Medicine
Trans. AMMM, Vol 1, No 1, 2019, Article ID S03P07

Infinite Science | Publishing

3D-printed standardized phantoms for small animal PET and MRI: a comparison study

F. Zell[1*], J. G. Mannheim[2], M. Grehn[1,3], and M. Rafecas[1]

[1] *Institute of Medical Engineering, University of Lübeck, Germany*
[2] *Department of Preclinical Imaging and Radiopharmacy, Eberhard Karls University Tuebingen, Germany*
[3] *Klinik für Strahlentherapie, Universitätsklinikum Schleswig-Holstein, Lübeck, Germany.*
[*] *Corresponding author, email: zell@imt.uni-luebeck.de*

Abstract: Three-dimensional (3D) printed phantoms are a cost-effective way for quality control of imaging devices. Here we evaluate two 3D printed versions of the NEMA NU 4-2008 phantom for small animal positron emission tomography (PET), compared to a phantom made of PMMA. The behavior of the materials is analyzed using PET for two radiotracers with different positron ranges, as well as the compatibility of the phantoms with MRI. In conclusion, image degradation due to positron range is more pronounced for the material E-Shell 600 clear. *Some support materials required by 3D printing can potentially produce artifacts in MRI images.*

I. Introduction

Standardized phantoms are required in medical imaging to assess the performance and quality control of imaging devices. 3D printing can be a fast and cost-effective alternative to build such phantoms, as long as their imaging properties are the same as for reference standard phantoms. The goal of this work was to evaluate the suitability of 3D printed phantoms for image quality (IQ) assessment in small animal positron emission tomography (PET), according to the NEMA NU 4-2008 standards [1]. Magnetic resonance imaging (MRI) data were also acquired, since combined PET/MRI systems are more and more used. The MRI data are usually co-registered with the PET images; therefore, potential distortions of the MRI images due to the printing materials were evaluated as well.

II. Material and methods

Three copies of the NEMA IQ phantom [1] were constructed. This phantom consists of three parts, see Fig.1: (1) A Recovery Coefficient (RC) region with 5 fillable rods with diameters from 1 to 5 mm to determine recovery coefficients; (2) a cylindrical volume filled with activity to determine the uniformity and noise characteristics, and (3) a region with two chambers filled with air and non-radioactive water ("cold region") to determine spill-over ratios (SORs), respectively. *Phantom 1* was printed using $ProJet^{®}3510$ *HDPlus* (material: $VisiJet^{®}X$). As reference, *Phantom 2* was manufactured using polymethylmethacrylate (PMMA), as indicated in the NEMA NU 4-2008 protocol. Additionally, the printer $Perfactory^{®}3$ *Mini Multi Lens* and the material *E-Shell 600 clear* were employed to print *Phantom 3*. For the two printed phantoms, the three parts were printed separately and glued together; their tightness was tested using a water-ink mixture. List-mode data were acquired with an Inveon dedicated PET system (Siemens Healthineers, Knoxville, TN, USA) using ^{18}F as committed by the NEMA protocol and data were acquired for 20 min at an injected activity of 3.7 MBq.

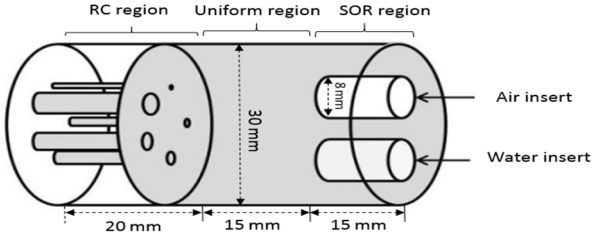

Figure 1: Sketch of the IQ phantom based on [3]. Areas filled with radioactivity are marked in gray.

The radiotracer ^{68}Ga was also used to evaluate the effects of positron range on the PET images in relation to the printing material. The attenuation properties were previously examined using computer tomography (CT) and were very similar. PET data were histogrammed and reconstructed without attenuation correction using filtered backprojection (FBP), with a pixel size of ~$(0.8\text{mm})^3$, ramp filter (0.5 Nyquist cut off), Fourier rebinning, and an ordered subset expectation maximization (OSEM3D) combined with a maximum a posteriori (MAP) algorithm with 2 OSEM3D and 18 MAP iterations, 16 OSEM3D subsets and a beta smoothing factor of 0.1mm. Following [1], we determined RCs, SOR and uniformity. First, an average image was generated containing the central 10 mm length of the rods; circular regions-of-interest (ROIs) with a diameter twice of each rod were drawn for each rod, and line profiles in axial direction were determined along the maximum ROI value. RC was calculated for each rod as the ratio of the average of each line profile and the average image intensity in the uniform region. To calculate the SOR, a volume-of-interest (VOI) was drawn in each cold chamber. SOR was defined as the ratio of the mean intensity in each cold region to the mean of the uniform area. The ideal values of RC and SOR are 1 and 0, respectively. To further examine the impact of the positron range on the reconstructed image, the full width at half maximum (FWHM) of the uniform region was determined. Additionally, MRI data were acquired with 3T MRI scanner (Philips Ingenia, Germany) using a T1

DOI: 10.18416/AMMM.2019.1909S03P07

spin echo sequence with a pixel size of 0.6mm^2 and a slice thickness of 3mm.

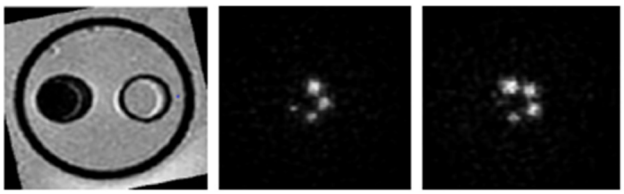

Figure 2: MRI image of Phantom 1 with a chemical shift (left). RC-region of Phantom 1 (middle) and Phantom 3 (right) filled with ^{68}Ga. Both images were reconstructed using OSEM3D.

III. Results and discussion

Only small weight differences between the phantoms were measured (see Table 1). The density was 1.18, 1.19 and 1.20 g/cm^3 for *Phantoms 1, 2* and *3*, respectively. *Phantom 1* dimensions, measured with a caliper, fulfilled the NEMA protocol, which only allows deviations smaller than 0.1 mm. In contrast length, height and diameter of *Phantom 3* differed up to 0.4 mm. The manufactured phantom corresponded exactly to the planning dimensions. The surfaces of *Phantom 1* were rougher due to the printer layers, which caused the creation of small air bubbles when filling with water/activity. Concerning their tightness, no coloration of the materials was visible after 17 h.

Table 1: Overview of the measured weights.

Weight	*Phantom 1*	*Phantom 2*	*Phantom 3*
Empty	40.91 g	40.75 g	41.55 g
Filled	61.50 g	61.45 g	62.61 g

In a study based on a preclinical PET/CT using ^{18}F [2], the authors concluded that the imaging characteristics of commercial phantoms and 3D printed replica were equivalent. In our case, some differences were observed, e.g. when using ^{68}Ga, and OSEM3D (see Fig. 2, right and middle); the differences were less pronounced for FBP images (Figs. 3 and 4), probably due to the inferior image quality inherent to the algorithm. Data from *Phantom 2* filled with ^{18}F appeared to have artifacts, so that corresponding images were excluded from the following analysis. As expected, SOR and RC worsened when compared to ^{18}F images due to the larger positron range of ^{68}Ga. Interestingly, the blurring was more pronounced for *Phantom 3*. This fact points out to a larger range of positrons in *E-Shell 600 clear* compared to the other printing materials. The reconstructed FWHM is in agreement with this observation and the tracer's positron range. The FWHM for *Phantom 1* and *Phantom 2* were within the expected range of 30 mm for both radiotracers, *Phantom 3* showed a larger width (31.83 mm) compared to ^{18}F (29.50 mm). In spite of the poorer image quality, *Phantom 3* yielded the best RC values for ^{68}Ga, compared to *Phantom 1* and *2*. In general, the latter two performed similarly. In preliminary investigations using MRI, *Phantom 1* showed irregularities on the edges and air bubbles. In the region of chambers emerged a ring artefact that indicates a chemical shift (Fig. 2, left), probably caused by the waxy support material of the 3D printer. In repeated MRI measurements, such artifacts were not visible. The support material might have dissolved or was removed after the phantom was filled and emptied several times.

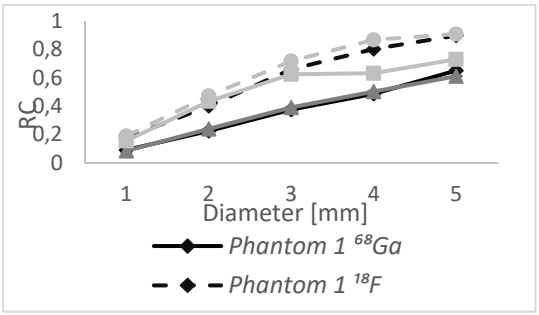

Figure 3: Recovery Coefficient (RC) for each rod.

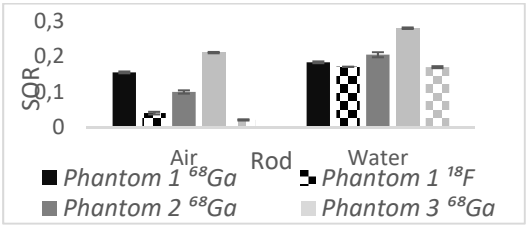

Figure 4: Spill-over ratio (SOR) for air and water.

IV. Conclusions

3D printed phantoms are cost-effective and flexible in design compared to commercial ones. This allows e.g. patient-specific applications. In this work, we show that a careful choice of the printing material is recommended. We have observed differences in the reconstructed images that might be attributed to the printing material. To disentangle the contribution of measurement and evaluation uncertainties behind the observed differences, further measurements are necessary. As the goal of the IQ phantom is to evaluate the performance and quality of a scanner or a reconstruction algorithm, effects due to the manufacturing procedure should be kept minimal. Attention should be also put on guaranteeing a stopping power for positrons similar to PMMA and avoiding rough inner surfaces.

Acknowledgments

We would like to thank R. Schulz (Scientific Workshop, University of Lübeck), and D. Wendt (Frauenhofer EMB).

Author's statement

The authors state no funding involved and no conflict of interest. Informed consent has been obtained from all individuals included in this study.

References

[1] National Electrical Manufacturers Association, *NEMA Standards Publication NU 4-2008, Performance Measurements of Small Animal Positron Emission Tomographs*, USA, 2008.

[2] M. F. Bieniosek, B. J. Lee and C. S. Levin, *Characterization of custom 3D printed multimodality imaging phantoms,* Medical Physics 42.10, pp.5913-5918, 2015.

[3] N. Anizan, et al., *Acquisition setting optimization and quantitative imaging for 124 I studies with the Inveon microPET-CT system,* EJNMMI research 2, pp. 7, 2012.